Published in final edited form as:

Mol Carcinog. 2016 May ; 55(5): 563–574. doi:10.1002/mc.22303.

Keratinocyte p38δ loss inhibits Ras-induced tumor formation, while systemic p38δ loss enhances skin inflammation in the early phase of chemical carcinogenesis in mouse skin

Alexi Kiss[1], **Aaron C. Koppel**[1], **Joanna Anders**[2], **Christophe Cataisson**[2], **Stuart H. Yuspa**[2], **Miroslav Blumenberg**[3], and **Tatiana Efimova**[1]

[1]Division of Dermatology, Washington University School of Medicine, St. Louis, Missouri, USA

[2]Laboratory of Cancer Biology and Genetics, National Cancer Institute, National Institutes of Health, Bethesda, Maryland, USA

[3]R. O. Perelman Department of Dermatology, NYU School of Medicine, New York, New York, USA

Abstract

p38δ expression and/or activity are increased in human cutaneous malignancies, including invasive squamous cell carcinoma (SCC) and head and neck SCC, but the role of p38δ in cutaneous carcinogenesis has not been well-defined. We have reported that mice with germline loss of *p38δ* exhibited a reduced susceptibility to skin tumor development compared with wild-type mice in the two-stage 7,12-dimethylbenz(*a*)anthracene (DMBA)/12-*O*-tetradecanoylphorbol-13-acetate (TPA) chemical skin carcinogenesis model. Here we report that *p38δ* gene ablation inhibited the growth of tumors generated from v-ras^{Ha}-transformed keratinocytes in skin orthografts to nude mice, indicating that keratinocyte-intrinsic p38δ is required for Ras-induced tumorigenesis. Gene expression profiling of v-ras^{Ha}-transformed p38δ-null keratinocytes revealed transcriptional changes associated with cellular responses linked to tumor suppression, such as reduced proliferation and increased differentiation, cell adhesion, and cell communications. Notably, a short-term DMBA/TPA challenge, modeling the initial stages of chemical skin carcinogenesis treatment, elicited an enhanced inflammation in p38δ-null skin compared with skin of wild-type mice, as assessed by measuring the expression of pro-inflammatory cytokines, including IL-1β, IL-6, IL-17, and TNFα. Additionally, p38δ-null skin and p38δ-null keratinocytes exhibited increased p38α activation and signaling in response to acute inflammatory challenges, suggesting a role for p38α in stimulating the elevated inflammatory response in p38δ-null skin during the initial phases of the DMBA/TPA treatment compared with similarly treated p38δ$^{+/+}$ skin. Altogether, our results indicate that p38δ signaling regulates skin carcinogenesis not only by keratinocyte cell-autonomous mechanisms, but also by influencing the interaction between the epithelial compartment of the developing skin tumor and its stromal microenvironment.

Correspondence: Dr. Tatiana Efimova, Division of Dermatology, Department of Internal Medicine, Washington University School of Medicine, Campus Box 8123, 660 S. Euclid Avenue, St. Louis, MO 63110, Telephone: 314-454-8547, Fax: 314-362-8159, tefimova@dom.wustl.edu.

Keywords

p38δ; knockout mice; orthotopic skin grafts; skin inflammation; p38α

Introduction

Epithelial cancers comprise over 90% of human cancers. Cutaneous SCC is the second most common cancer in the United States, and exhibits poor prognosis in advanced stages [1]. Since activating mutations in ras genes are highly prevalent in human cancers, including SCCs, an improved understanding of the signaling pathways mediating ras-driven epithelial carcinogenesis is desirable. Among the best characterized ras downstream effector pathways are those including mitogen-activated protein kinase (MAPK) pathways. The MAPKs are evolutionarily conserved families of serine/threonine kinases that control diverse cellular processes in response to extracellular stimuli [2–4]. The p38 MAPK subfamily consists of p38α, p38β, p38γ, and p38δ isoforms, which are activated by environmental stressors, inflammatory cytokines, and growth factors to regulate, in a context-specific manner, cell proliferation, differentiation, transformation, senescence, migration, and inflammation [4]. Consistent with the importance of these cellular processes in tumorigenesis, p38 signaling is implicated in cancer development (reviewed in [5]). However, the specific functional contributions of individual p38 isoforms to epithelial carcinogenesis have not been fully elucidated.

The p38δ isoform is abundant in cutaneous epithelia (reviewed in [6]). p38δ expression is upregulated in invasive human SCC and in liver cancer, and activated p38δ is associated with head and neck SCC, suggesting a role for p38δ in human epithelial cancer development [7–9]. We have reported that systemic (germline) p38δ deletion results in a significant protection against skin tumor development in a two-stage DMBA/TPA chemical mouse skin carcinogenesis model, indicating that p38δ positively regulates tumorigenesis [10]. However, the molecular mechanisms underlying p38δ functions in this regulation, and the potential functional contributions of keratinocyte-derived and non-epithelial (i.e. myeloid, endothelial or stromal fibroblast) cell-derived p38δ to skin carcinogenesis remain to be determined.

The two-stage DMBA/TPA chemical skin carcinogenesis model involves both the DMBA-induced early initiation of activating mutations in the Harvey rat sarcoma (Ha-ras) gene, and tumor-promoting inflammation stimulated by the recurrent exposure of the skin to TPA. Here we employed both oncogenic transformation of keratinocytes, and the two-stage DMBA/TPA model, to examine the epithelial-intrinsic factors, as well as the inflammatory mediators that may interact to influence skin tumorigenesis. To compare the *in vivo* potential for tumor formation of p38δ-null versus wild-type keratinocytes in response to activated Ha-ras, we first assessed tumorigenicity of p38δ-null keratinocytes expressing an oncogenic v-ras^{Ha} in nude mouse skin grafts. Next, to investigate the transcriptional effects of p38δ deficiency on the early stages of ras transformation, we analyzed global expression profiles of v-ras^{Ha}-transformed control and p38δ-null keratinocytes. Last, we examined the effects of systemic p38δ gene ablation on the initial inflammatory response in the skin of mice

subjected to a short-term DMBA/TPA challenge. Our results reveal that p38δ contributes both cell-autonomous and paracrine effects during the course of skin tumor formation.

Materials and Methods

Reagents and Antibodies.

DMBA, TPA, bromodeoxyuridine (BrdU), Hoechst 33342, p38α, and β-actin antibodies were purchased from Sigma (St. Louis, MO). phosho-p38 antibody was from Cell Signaling Technology (Danvers, MA). BrdU antibody was from Chemicon (Temecula, CA). p38δ antibody was purchased from the Division of Signal Transduction Therapy (Dundee, UK) [11].

Mice.

All animal studies were approved by the Washington University School of Medicine (WUSM) Animal Studies Committee. Mice were housed under pathogen-free conditions according to the guidelines of the Division of Comparative Medicine, WUSM. Generation of mice with germline deletion of *p38δ* ($p38\delta^{-/-}$) was previously reported [12]. The mice were on a C57BL/6 genetic background. Genotyping was performed as described [12].

Nude mouse grafting.

$p38\delta^{+/+}$ and $p38\delta^{-/-}$ primary newborn mouse keratinocytes grown in medium with 0.05 mM calcium were infected with the v-ras^{Ha} retrovirus on day 3 in culture, trypsinized and used for grafting on day 8 as described [13,14].

Blood vessel density assessment in papillomas.

As a reflection of intra-tumoral angiogenesis, we measured blood vessel areas (μm^2) per 1×10^4 μm^2 stroma area in tumors developed from v-ras^{Ha}-transformed $p38\delta^{+/+}$ and $p38\delta^{-/-}$ keratinocytes as follows: intra-tumoral stroma areas adjacent to the epithelial-stromal interface were randomly demarcated on H&E-stained tumor sections viewed at 10x magnification, using the polygon selection tool in ImageJ. (Tumor sections adjacent to those stained with H&E were additionally immunostained for CD31 antigen outlining blood vessels within tumors (Supplementary Figure S1), to confirm the blood vessel localization patterns observed on the H&E-stained tumor sections.) Blood vessel areas were then measured, pooled, and averaged for each tumor sample. Data are reported as mean ± SE; n = 4 ($p38\delta^{+/+}$ tumors), n = 3 ($p38\delta^{-/-}$ tumors). Two to four 10x images per tumor, and two to three measurements per each 10x image were included in the analysis. $^*P < 0.05$, Mann-Whitney test, one-tailed.

RNA isolation and microarray analysis.

Total RNA extraction from mouse keratinocyte samples, and the assessment of the integrity, purity and quantity of RNA samples were performed as described [15]. Illumina Mouse6 BeadChip microarray assays were performed at the Washington University Genome Technology Access Center microarray facility according to the manufacturer's protocol. Primary keratinocytes were isolated from two wild-type ($p38\delta^{+/+}$), two heterozygous (p38δ

$^{+/-}$) and four p38δ knockout (p38δ$^{-/-}$) newborn mice. Keratinocytes from the p38δ$^{+/+}$ and the p38δ$^{+/-}$ individual samples were then combined to comprise a p38δ$^{+/+}$/ p38δ$^{+/-}$ pooled sample. Keratinocytes from the individual p38δ$^{-/-}$ samples were combined to comprise a p38δ$^{-/-}$ pooled sample. p38δ$^{+/+}$/ p38δ$^{+/-}$ (referred to as control) and p38δ$^{-/-}$ cells, plated in triplicates, were mock-infected or infected with the v-ras^{Ha} retrovirus on day 3 in culture, and harvested for RNA extraction at 4 days post-infection. Microarray data analysis was performed as described [15,16]. We used DAVID for gene ontology investigation. In the annotation chart we chose categories statistically significant with p-values less than 10^{-4} for regulated genes. Because DAVID charts contain redundant categories flagged from multiple data banks, we also presented clusters, which represent categories with largely overlapping genes; we included clusters with enrichment factors of 1.98 or better, and each cluster comprised representative ontological categories.

A short-term DMBA/TPA treatment.

DMBA (100 μg in 200μl acetone per mouse) or acetone vehicle was topically applied to shaved dorsal skin of sets of 12–15 weeks old p38δ$^{+/+}$ and p38δ$^{-/-}$ littermates two days after shaving. Starting five days after DMBA treatment, mice were topically treated every other day with four applications of TPA (12.5 μg in 200 μl acetone per mouse per each dose) or vehicle. Full-thickness dorsal skin samples were collected at the indicated time point after the final TPA application for subsequent analyses.

qRT-PCR.

qRT-PCR was performed using cDNA template made from total RNA extracted from full-thickness mouse skin samples using TRIzol reagent as recommended by the manufacturer (Invitrogen, Carlsbad CA), followed by additional purification with the RNA cleanup protocol of the RNeasy Mini Kit (Qiagen, Valencia CA). The cDNA template was produced using the Applied Biosystems High Capacity cDNA Archive Kit (Applied Biosystems, Foster City CA). qRT-PCR was performed using Fast SYBR Green Master Mix (Applied Biosystems by Life Technologies, Carlsbad CA), and the amplification was performed in quadruplicates using the fast mode (annealing and extending at 60 °C) of the ViiA7 Fast Real-Time PCR system (Applied Biosystems by Life Technologies). The comparative Ct (threshold cycle) method (ΔΔCt) was used for relative quantification of gene expression, with TATA-binding protein (Tbp) as a reference gene. Statistical analysis was performed using a two-tailed, unpaired Student's t-test (PRISM software, Graph Pad Software Inc., La Jolla, CA). Differences were considered significant when the *P* value was <0.05. The primers were designed for SYBR Green qRT-PCR chemistry using the Primer3 primer design tool at http://frodo.wi.mit.edu/primer3. The primer sequences are listed in Supplementary Table S1.

Cell culture, transient transfection and lucifearase assay.

Primary mouse epidermal keratinocytes were isolated from newborn (day 0) mice, cultured, and transfected using FuGENE HD Transfection Reagent (Roche Diagnostics GmbH, Mannheim, Germany) as described [15]. Each dish was transfected with pGL4.32[luc2P/NF-κB-RE/Hygro] vector that contains five copies of an NF-κB response element (NF-κB-RE) that drives transcription of the luciferase reporter gene (Promega, Madison WI). After 48

hours, the cells were starved of EGF for an additional 24 h, pretreated or not with 10μM SB203580 for 1 hour, and then stimulated with 100 ng/ml TNFα for 6 hours, harvested and assayed for luciferase activity using Luciferase Assay System (Promega) and Lumat LB 9507 luminometer (Berthold Technologies). Assays were performed in triplicates. Two independent experiments were performed using keratinocytes isolated from newborn epidermis of sets of individual littermates (n=4 per each genotype per experiment), pooled prior to plating. Total soluble protein concentration of the cell lysates was determined using Bradford Protein Assay reagent (Bio-Rad, Hercules, CA). Luciferase activity was normalized per μg of protein as described [17]. Statistical data analysis was performed using two-tailed unpaired t tests, with P values <0.05 considered to be significant.

Tissue protein isolation, ELISA and immunoblot analysis.

Full-thickness dorsal skin samples were collected, protein lysates were obtained, and protein concentration of the lysates was determined as previously reported [10]. IL-1β, IL-6, and TNFα levels in the full-thickness skin lysates were measured using the appropriate R&D Systems DuoSet ELISA Kits according to the manufacturer's recommendation (R&D Systems, Minneapolis, MN). ELISA reactions from each sample were measured in duplicates. Tissue cytokine levels were determined by normalizing the interpolated cytokine amounts to the total protein concentration of the respective sample and expressed as pg cytokine/μg protein for each skin lysate sample. Normalized skin tissue cytokine levels between experimental animal groups of different genotypes were compared using ANOVA, and pair-wise comparisons were performed using two-tailed, unpaired Student's t-test (PRISM software, Graph Pad Software Inc.) to determine statistically significant differences. Immunoblot analysis was performed as described [10].

Histology and immunofluorescence.

Tumor samples and dorsal skin samples were processed as previously detailed [10,15]. Histological and immunofluorescence analyses were performed as decribed [15].

Statistical Analysis.

The statistical methods employed to analyze the data resulting from the specific experimental procedures are detailed in the corresponding paragraphs describing those procedures. Data were deemed to be statistically significant if the P-values were < 0.05.

Results

p38δ deficiency inhibits growth of squamous tumors generated from v-ras^{Ha}-transformed keratinocytes following skin grafting onto nude mice.

DMBA-induced activating mutations in the Ha-ras gene are found in tumors arising from DMBA/TPA treatment [18]. To evaluate if deficient tumor development in response to activated Ha-ras in p38δ-null keratinocytes is a cell autonomous function, p38δ$^{+/+}$ and p38δ$^{-/-}$ primary keratinocytes were transduced with v-ras^{Ha} retrovirus, transplanted onto nude mice, and the growth of v-ras^{Ha}-induced tumors in the presence and absence of keratinocyte-specific p38δ was compared. Tumor growth was significantly diminished in the absence of keratinocyte-specific p38δ relative to that of tumors formed by p38δ$^{+/+}$ keratinocytes at all

time points during the course of the study (Figure 1A). The tumors arising from keratinocytes of both genotypes were histologically characterized as squamous papillomas (Figure 1B). Papillomas developing from p38δ-null v-ras^{Ha}-transformed keratinocytes exhibited significantly reduced proliferation, compared with that in tumors from p38δ$^{+/+}$ v-ras^{Ha}-transformed keratinocytes, as measured by BrdU staining (Figure 1C and D). Furthermore, while the proliferating BrdU-positive cells in tumors arising from p38δ$^{+/+}$ keratinocytes were localized both in the basal and the suprabasal epithelial compartments (a hallmark of tumors at high risk for malignant conversion), the proliferating cells in tumors from p38δ-null keratinocytes were largely restricted to the basal compartment (Figure 1C, insets), a typical feature of tumors at low risk for malignant conversion [19]. These results are consistent with our previous finding that DMBA/TPA-induced papillomas in mice with systemic p38δ ablation exhibited reduced proliferation and reduced size compared with those in wild-type mice [10]. In addition, papillomas derived from p38δ-null v-ras^{Ha}-transformed keratinocytes were less highly vascularized, compared with papillomas from p38δ$^{+/+}$ keratinocytes (Figure 1E), indicating that angiogenic response was negatively affected by keratinocyte p38δ loss. This is in agreement with the transcriptional down-regulation of functionally related genes in the “blood vessel development”/”vasculature development” categories in p38δ-null v-ras^{Ha}-transformed keratinocytes, as revealed by gene expression profiling (Tables 1 and 2B, discussed below).

Overall, these data show that keratinocytes lacking p38δ displayed an impaired capacity to promote growth of v-ras^{Ha}-induced orthotopic squamous tumors, indicating that keratinocyte-intrinsic p38δ functionally contributes to Ras-induced tumorigenesis.

Gene expression profiling of p38δ-null v-ras^{Ha}-transformed keratinocytes reveals transcriptional changes linked to cellular responses that contribute to tumor suppression.

To identify genes regulated by p38δ during the early stages of oncogenic ras-induced transformation in keratinocytes, we analyzed global gene expression in v-ras^{Ha}-transformed control and p38δ-null keratinocytes by microarray analysis. We defined differentially expressed genes as those with at least 50% higher average expression in the p38δ-null keratinocytes (induced), or in the control cells (suppressed) (Supplementary Table S1). Selected genes differentially expressed between v-ras^{Ha}-transformed p38δ-null and v-ras^{Ha}-transformed control keratinocytes, grouped into ontological categories, are shown in Table 1 and Supplementary Table S3. Gene expression differences for selected genes were validated by qRT-PCR. For example, fliaggrin (FLG), hornerin (HRNR), repetin (RPTN), and late cornified envelope 1L (LCE1L) expression was up-regulated by 2.4-, 2.6-, 1.8-, and 22.3-fold, respectively, in v-ras^{Ha}-transformed p38δ-null relative to control keratinocytes, by qRT-PCR. Analysis of the ontological categories of the regulated genes revealed that the expression of the genes linked to keratinocyte differentiation, cell adhesion, and cell communications (i.e. gap junction, ion channel) was up-regulated, while the expression of the genes linked to cell proliferation and growth factor-induced receptor protein tyrosine kinase signaling was down-regulated by p38δ ablation in v-ras^{Ha}-induced transformation (Table 1, Supplementary Tables S2, S3). Functional annotation clustering analysis using the cutoff enrichment score of > 1.98 showed that the “keratinization”, “epidermal cell differentiation”, “ion channel activity”, “cell adhesion”, and “gap junction” clusters were

significantly enriched among the groups of up-regulated genes (Table 2A). In the down-regulated clusters, “EGF-like”, “transmembrane receptor protein tyrosine kinase activity”, and “blood vessel development” groups, among others, were significantly enriched (Table 2B).

These results suggest that during the early stages of oncogenic transformation, p38δ ablation in keratinocytes causes transcriptional changes associated with cellular responses that contribute to tumor suppression, such as reduced proliferation and angiogenesis, as well as increased differentiation, cell adhesion, and cell communications [20].

Skin of p38δ-null mice displays an augmented induction of inflammatory mediators in response to a short-term DMBA/TPA regimen compared with skin of similarly treated wild-type littermates.

To characterize the impact of global p38δ ablation on early DMBA/TPA-induced inflammatory response in skin, we analyzed the levels of inflammatory mediators in the skin of p38δ$^{+/+}$ and p38δ$^{-/-}$ mice after subjecting them to a short-term DMBA/TPA regimen. qRT-PCR analysis revealed significantly over-induced mRNA levels of the inflammatory cytokines TNFα, IL-1β, IL-6 and IL-17, and the damage-associated molecular pattern (DAMP) molecules or “alarmins” S100A8 and S100A9 in p38δ$^{-/-}$ skin compared with control p38δ$^{+/+}$ skin subjected to the inflammatory challenge described above (Figure 2A, Supplementary Table S4). Additionally, analysis of the cytokine production by ELISA demonstrated a significantly higher induction of TNFα, IL-1β, and IL-6 proteins in the DMBA/TPA-treated p38δ$^{-/-}$ skin relative to the similarly-treated p38δ$^{+/+}$ skin (Figure 2B). In contrast, the DMBA/TPA-stimulated mRNA induction of several additional regulators and markers examined, such as IL-10, TGFβ, TSLP, VEGF-A, Filaggrin and Lce1l, did not differ between p38δ$^{+/+}$ and p38δ$^{-/-}$ skin (Figure 2A,Supplementary Table S4). The lack of differences between p38δ-null and wild-type skin in the DMBA/TPA-stimulated induction of TSLP (a sensitive measure of the epidermal barrier integrity) [21] and Filaggrin and Lce1l (epidermal differentiation markers) expression suggests that the exacerbated inflammatory response displayed by the p38δ-null skin was not due to an impaired barrier formation or an epidermal differentiation defect in the mutant skin.

Among additional features indicative of the exacerbated skin inflammation, Munro microabscesses, intraepidermal inflammatory infiltrates, and a significantly higher degree of epidermal thickening were observed in the DMBA/TPA-treated p38δ-null, but not in p38δ$^{+/+}$ skin (Figure 2C-F). Collectively, these results show that systemic p38δ deficiency leads to an increased initial inflammatory response in the pre-neoplastic skin of mice subjected to a short-term DMBA/TPA challenge.

Enhanced activation of p38α signaling in p38δ$^{-/-}$ skin in response to a short-term DMBA/TPA regimen, and in p38δ$^{-/-}$ keratinocytes in response to TNFα.

The p38 isoforms have been implicated in the regulation of inflammatory cytokine expression (reviewed in [4]). p38α and p38δ are the predominant p38 isoforms expressed in epidermis (reviewed in [6]). We therefore examined whether p38δ loss influenced the activation of p38α in response to inflammatory challenges. By immunoblot, we assessed the

phosphorylated (active) and total p38α and p38δ levels in protein extracts isolated from full-thickness skin of groups of p38δ$^{+/+}$ and p38δ$^{-/-}$ mice following the short-term DMBA/TPA regimen. Because the phospho-specific antibody against p38 reacts with the phosphorylated form of all p38 isoforms, and p38α and p38δ are the two most abundant p38 isoforms in skin, the phospho-p38 (p-p38) immunoreactive band in Figure 3A reflected the activation of both p38α and p38δ in p38δ$^{+/+}$ skin, and of p38α only in p38δ-depleted (p38δ$^{-/-}$) skin. As shown in Figures 3A and B, p38α activation in response to a short-term DMBA/TPA challenge was hyper-induced in p38δ$^{-/-}$ relative to p38δ$^{+/+}$skin. We also observed a higher level of p38α activation in TNFα-treated mouse p38δ$^{-/-}$ keratinocytes, compared with that in similarly-treated p38δ$^{+/+}$ keratinocytes (Figure 3C).

p38α regulates cytokine production by controlling the activities of several transcription factors, including that of NF-κB, a key regulator of cytokine gene transcription [4,22,23]. We next measured NF-κB transcriptional activity in TNFα-stimulated p38δ$^{+/+}$ and p38δ$^{-/-}$ mouse keratinocytes, using a NF-κB reporter construct. As shown in Figure 3D, the degree of TNFα-induced NF-κB activation was significantly higher in p38δ$^{-/-}$ relative to p38δ$^{+/+}$ cells. This hyper-augmentation in NF-κB transcriptional activity in p38δ$^{-/-}$ cells was abrogated by a pre-treatment with SB203580, the inhibitor selective for p38α/p38β isoforms (Figure 3D). Because p38β protein expression was undetectable in either wild-type or p38δ-null cultured mouse keratinocytes (data not shown), this finding indicates that the observed increase in the TNFα-stimulated NF-κB activation in p38δ-null cells compared with that in wild-type cells is p38α-dependent. Notably, in p38δ$^{+/+}$ keratinocytes, TNFα-induced NF-κB activation is insensitive to p38α inhibition by SB203580, indicating that p38α does not contribute to TNFα-dependent NF-κB transcriptional activity in wild-type keratinocytes (Figure 3D). In contrast, in p38δ-null cells, p38α contribution to TNFα-dependent NF-κB transcriptional activity is significant, and accounts for approximately one-third of the promoter activity induction by TNFα, compared with that in wild-type keratinocytes (Figure 3D). Since JNK1/2 also contribute to TNFα-induced NF-κB activation in keratinocytes [22], TNFα-stimulated JNK1/2 activity may account for the residual TNFα-dependent NF-κB transcriptional activity in SB203580-treated p38δ$^{-/-}$ cells. Moreover, potential involvement of additional signaling kinases in this regulation cannot be excluded; further studies will address this possibility.

Altogether, these findings suggest that increased p38α signaling in the settings of p38δ deficiency underlies the exacerbated inflammatory cytokine production in pre-neoplastic skin during the initial phases of the DMBA/TPA regimen.

Discussion

Consistent with our previous finding that mice lacking p38δ are significantly protected from chemically-induced skin tumor development [10], here we showed that p38δ-deficient keratinocytes have an impaired capacity to promote growth of oncogenic ras-induced squamous tumors following orthotopic skin grafting onto nude mice. When v-ras^{Ha}-transformed p38δ-deficient keratinocytes were grafted onto p38δ-intact hosts, tumor growth was significantly diminished, and proliferation of tumor cells was reduced, with the majority of proliferative cells restricted to the basal epithelial compartment, a pattern typically

detected in low-risk papillomas [19]. Notably, DMBA/TPA-induced tumors harvested from p38δ-null mice likewise showed reduced size and reduced number of proliferative tumor cells localized to the basal layer [10], demonstrating that the functional effect of p38δ loss on the appearance of skin tumors is similar in the two different models of mouse skin carcinogenesis. Our present findings thus indicate that keratinocyte-intrinsic p38δ functionally contributes to ras-induced tumorigenesis as a downstream effector in the oncogenic Ha-ras pathway, by regulating tumor cell proliferation in a cell-autonomous manner.

Nevertheless, the involvement of the non-epithelial cell-derived p38δ in skin tumorigenesis cannot be excluded, since p38δ is expressed in many cell types, including immune, endothelial, and mesenchymal cells (reviewed in [6]), interplay of which with epithelial cells is known to be of key importance for tumor development and progression [24,25]. Importantly, studies targeting p38α isoform in distinct cell types have revealed cell type-specific effects of p38α loss on inflammatory and allergic responses in skin, and on inflammatory bowel disease [26–28]. The effects of keratinocyte-specific and myeloid cell-specific p38δ loss on distinct stages of chemical skin carcinogenesis are under investigation in our laboratory.

The *in vivo* mouse skin and lung carcinogenesis studies, as well as the studies involving human cutaneous and liver malignancies have suggested a tumor-promoting role for p38δ [7–10]. Conversely, the reports using cultured mouse or human fibroblasts showed that p38δ loss was associated with impaired contact inhibition or abrogation of oncogenic ras-induced senescence, respectively [29,30], implying potential tumor-suppressing roles for p38δ in these experimental systems. Collectively, these findings argue that the functional contributions of p38δ to cancer phenotypes are context-dependent. Of note, recent studies have revealed opposing effects on skin tumorigenesis of epidermal-specific and dermal fibroblast-specific deletion of RBPj, a downstream effector of Notch signaling. Thus, the epidermal-specific RBPj loss elicits a tumor-suppressing response [31], whereas RPBj-deficient fibroblasts have tumor-enhancing effects [32]. These data underscore the importance of cell-selective targeting of the potential disease modulators.

Using global gene expression profiling, we have established that during the early stages of ras-induced tumorigenesis, the oncogenic ras-p38δ-null phenotype is characterized by transcriptional changes associated with cellular mechanisms that negatively regulate tumorigenesis, such as reduced cell proliferation and angiogenesis, and increased cell differentiation, cell adhesion and cell communications [20]. Notably, tumor formation from grafted murine papilloma cells was reduced by treatment of grafts with a differentiation-inducing agent [33]. Oncogenic ras induces differentiation-like features in keratinocytes, including expression of differentiation marker genes [34–36]. Our microarray analysis showed that in p38δ-null keratinocytes, v-ras^{Ha} induced higher expression levels of the epidermal differentiation complex genes [37], including the cornified envelope precursors loricrin, small proline-rich proteins (SPRRs) and LCE genes, as well as the four members of the filaggrin-like gene family, filaggrin, repetin, hornerin, and filaggrin 2. These data suggest that a more differentiated phenotype of p38δ-null v-ras^{Ha}-transformed keratinocytes may

underlie, at least in part, an impaired capacity of these cells to promote tumor development, compared with that of the control v-ras^{Ha}-transformed keratinocytes.

Cell-cell contact and cell-cell communications are also important cellular mechanisms that contribute to tumor suppression by preserving tissue homeostasis and controlling behavior of initiated cells [38]. The latter interact with normal proliferating and differentiating cells in a stratified epithelium through an assortment of intercellular junctional complexes, including tight, adherence, desmosomal and gap junctions, and these interactions are required for normal cells to suppress the transformed phenotype (reviewed in [38]). Remarkably, a number of genes encoding proteins involved in cell-cell adhesion and gap junctional communications are up-regulated in p38δ-null v-ras^{Ha}-transformed keratinocytes (Table 1), indicating a potential for a more efficient suppression of the neoplastic phenotype by normal cells through reinforced communications with the initiated cells in p38δ-null skin. Of note, the desmosomal cadherin desmoglein 1, that is overexpressed in p38δ-null v-ras^{Ha}-transformed keratinocytes, in addition to its adhesive function, is also known to promote epidermal differentiation [39]. Unexpectedly, p38δ ablation resulted in the augmented oncogenic ras-induced expression of the genes in ontological categories for ion channels, including numerous genes encoding protein subunits of different potassium and sodium channels, among others (Tables 1 and 2). Given the growing appreciation of the important role for ion channels in regulation of balance between apoptosis and proliferation [40], further studies are needed to ascertain the functional importance of the altered expression of the specific ion channels for oncogenic ras-driven tumorigenesis.

Our present study showed that systemic p38δ deficiency led to an exacerbated initial inflammatory response in the pre-neoplastic skin of mice following a short-term DMBA/TPA challenge. p38α and p38δ are the predominant keratinocyte p38 isoforms. Our data revealed an enhanced activation of p38α signaling in p38δ-null keratinocytes in response to inflammatory stimuli both *in vitro* and *in vivo*, underscoring a compensatory interplay between the two main epidermal p38 isoforms. The functional implications of this interplay for epidermal development and disease remain to be elucidated. We argue that the hyper-activation of p38α signaling drives the enhanced inflammation in p38δ-null pre-neoplastic skin during the initial phases of the DMBA/TPA regimen. Our results suggest that p38α regulates the inflammatory cytokine over-production via a mechanism that involves over-induction of NF-κB transcriptional activity.

It is well-recognized that the immune system and a developing tumor may interact in a complex manner, whereby host immunity can engender either tumor-promoting or tumor-suppressing outcomes [41,42]. We theorize that the observed p38α-dependent hyperinflammation in the setting of systemic p38δ deficiency elicits anti-tumor immune responses by facilitating the recruitment to the skin of certain types of immune cells which function to mediate the resistance of p38δ-null mice to chemically-induced papilloma development. In support of this assertion, intestinal epithelial cell-intrinsic p38α contributes to the pathogen-induced host immune responses by mediating immune cell recruitment into the intestinal mucosa [43]. Notably, secreted “alarmins” S100A8 and S100A9, which are over-induced in inflamed p38δ-null skin (Figure 2A, Supplementary Table S4), are known to promote recruitment and activation of a wide range of immune cells. Further studies will

determine which specific types of infiltrating immune cells functionally contribute to the tumor-resistant phenotype afforded by the global p38δ ablation.

Remarkably, a correlation between heightened inflammatory response to short-term TPA or DMBA/TPA challenges and associated resistance to DMBA/TPA-induced papilloma formation has been detected in several mouse models, including mice lacking MSK1/2, the downstream effectors of ERK1/2 and p38 signaling [44]; mice with epidermal-specific HIF1α gain-of-function [45,46]; and triple knockout EPI−/− mice lacking envoplakin, periplakin, and involucrin genes [47]. Notably, the exacerbated inflammatory response to TPA in EPI−/− mice involved multiple immune cell types, and could not be normalized by suppressing single specific leukocyte subset [47]. Additionally, TSLP-dependent inflammation was reported to protect mice with epidermal-specific loss of Notch signaling from skin tumorigenesis through a direct effect on dermal T cells [31,48]. Furthermore, strains of mice selectively bred to achieve maximal acute inflammatory responsiveness exhibited resistance to the development of DMBA/TPA-induced skin tumors, and showed enhanced natural killer cell activity and increased production of pro-inflammatory cytokines [49,50]. Altogether, these findings underscore the functional contributions of immune/inflammatory components to the tumor-suppressing microenvironment during skin tumor development.

In summary, our results indicate that p38δ signaling regulates skin carcinogenesis not only by keratinocyte cell-autonomous mechanisms, but also by influencing the interaction between the epidermal and dermal compartments of the skin, as well as the cross-talk between the epithelial compartment of the developing skin tumor and its stromal microenvironment. Our present findings, in conjunction with our previous evidence for the importance of p38δ in promoting skin and lung tumorigenesis [10], and with recent report that highlighted the pro-tumorigenic role of p38δ (along with that of p38γ) in colitis-associated colon cancer [51], suggest potential therapeutic prospects by targeting p38δ for treatment of cancer. Future studies examining the effects of cell type-selective p38δ targeting at different stages of skin carcinogenesis in mice will elucidate the functional roles of p38δ in the specific cell types that participate in the tumorigenesis process, and will guide future therapeutic strategies.

Supplementary Material

Refer to Web version on PubMed Central for supplementary material.

Acknowledgments

We thank Dr. Brian Kim for critical reading of the manuscript and valuable comments.

Financial support: this work was supported by the National Institutes of Health grant R01 CA133038 (T.E.). Parts of this work were supported by the intramural program of the Center for Cancer Research of the National Cancer Institute (J.A., C.C., and S.H.Y.).

Abbreviations used:

SCC	squamous cell carcinoma

DMBA	7,12-dimethylbenz(*a*)anthracene
TPA	12-*O*-tetradecanoylphorbol-13-acetate
MAPK	mitogen-activated protein kinase
ERK	extracellular signal-regulated protein kinase
JNK	stress-responsive c-Jun NH2-terminal kinase
IL	interleukin
TSLP	thymic stromal lymphopoietin
BrdU	bromodeoxyuridine

References

1. Dlugosz A, Merlino G, Yuspa SH. Progress in cutaneous cancer research. J Investig Dermatol Symp Proc 2002;7:17–26.
2. Raman M, Chen W, Cobb MH. Differential regulation and properties of MAPKs. Oncogene 2007;26:3100–3112. [PubMed: 17496909]
3. Weston CR, Davis RJ. The JNK signal transduction pathway. Curr Opin Cell Biol 2007;19:142–149. [PubMed: 17303404]
4. Cuadrado A, Nebreda AR. Mechanisms and functions of p38 MAPK signalling. Biochem J 2010;429:403–417. [PubMed: 20626350]
5. Wagner EF, Nebreda AR. Signal integration by JNK and p38 MAPK pathways in cancer development. Nat Rev Cancer 2009;9:537–549. [PubMed: 19629069]
6. Efimova T p38delta mitogen-activated protein kinase regulates skin homeostasis and tumorigenesis. Cell Cycle 2010;9:498–505. [PubMed: 20090411]
7. Haider AS, Peters SB, Kaporis H, Cardinale I, Fei J, Ott J, et al. Genomic analysis defines a cancer-specific gene expression signature for human squamous cell carcinoma and distinguishes malignant hyperproliferation from benign hyperplasia. J Invest Dermatol 2006;126:869–881. [PubMed: 16470182]
8. Li-Sher FT, Ooi A, Huang D, Wong JC, Qian CN, Chao C, et al. p38delta/MAPK13 as a diagnostic marker for cholangiocarcinoma and its involvement in cell motility and invasion. Int J Cancer 2010;126:2353–2361. [PubMed: 19816939]
9. Junttila MR, la-aho R, Jokilehto T, Peltonen J, Kallajoki M, Grenman R, et al. p38alpha and p38delta mitogen-activated protein kinase isoforms regulate invasion and growth of head and neck squamous carcinoma cells. Oncogene 2007;26:5267–5279. [PubMed: 17334397]
10. Schindler EM, Hindes A, Gribben EL, Burns CJ, Yin Y, Lin MH, et al. p38delta Mitogen-activated protein kinase is essential for skin tumor development in mice. Cancer Res 2009;69:4648–4655. [PubMed: 19458068]
11. Sabio G, Reuver S, Feijoo C, Hasegawa M, Thomas GM, Centeno F, et al. Stress- and mitogen-induced phosphorylation of the synapse-associated protein SAP90/PSD-95 by activation of SAPK3/p38gamma and ERK1/ERK2. Biochem J 2004;380:19–30. [PubMed: 14741046]
12. Sabio G, Arthur JS, Kuma Y, Peggie M, Carr J, Murray-Tait V, et al. p38gamma regulates the localisation of SAP97 in the cytoskeleton by modulating its interaction with GKAP. EMBO J 2005;24:1134–1145. [PubMed: 15729360]
13. Lichti U, Anders J, Yuspa SH. Isolation and short-term culture of primary keratinocytes, hair follicle populations and dermal cells from newborn mice and keratinocytes from adult mice for in vitro analysis and for grafting to immunodeficient mice. Nat Protoc 2008;3:799–810. [PubMed: 18451788]

14. Cataisson C, Ohman R, Patel G, Pearson A, Tsien M, Jay S, et al. Inducible cutaneous inflammation reveals a protumorigenic role for keratinocyte CXCR2 in skin carcinogenesis. Cancer Res 2009;69:319–328. [PubMed: 19118017]
15. Lin C, Hindes A, Burns CJ, Koppel AC, Kiss A, Yin Y, et al. Serum response factor controls transcriptional network regulating epidermal function and hair follicle morphogenesis. J Invest Dermatol 2013;133:608–617. [PubMed: 23151848]
16. Lee DD, Zavadil J, Tomic-Canic M, Blumenberg M. Comprehensive transcriptional profiling of human epidermis, reconstituted epidermal equivalents, and cultured keratinocytes using DNA microarray chips. Methods Mol Biol 2010;585:193–223. [PubMed: 19908006]
17. Schindler EM, Baumgartner M, Gribben EM, Li L, Efimova T. The Role of Proline-Rich Protein Tyrosine Kinase 2 in Differentiation-Dependent Signaling in Human Epidermal Keratinocytes. J Invest Dermatol 2007;127:1094–1106. [PubMed: 17205062]
18. Balmain A, Ramsden M, Bowden GT, Smith J. Activation of the mouse cellular Harvey-ras gene in chemically induced benign skin papillomas. Nature 1984;307:658–660. [PubMed: 6694757]
19. Glick A, Ryscavage A, Perez-Lorenzo R, Hennings H, Yuspa S, Darwiche N. The high-risk benign tumor: evidence from the two-stage skin cancer model and relevance for human cancer. Mol Carcinog 2007;46:605–610. [PubMed: 17538943]
20. Hanahan D, Weinberg RA. Hallmarks of cancer: the next generation. Cell 2011;144:646–674. [PubMed: 21376230]
21. Demehri S, Liu Z, Lee J, Lin MH, Crosby SD, Roberts CJ, et al. Notch-deficient skin induces a lethal systemic B-lymphoproliferative disorder by secreting TSLP, a sentinel for epidermal integrity. PLoS Biol 2008;6:e123. [PubMed: 18507503]
22. Pastore S, Mascia F, Mariotti F, Dattilo C, Mariani V, Girolomoni G. ERK1/2 regulates epidermal chemokine expression and skin inflammation. J Immunol 2005;174:5047–5056. [PubMed: 15814736]
23. Freund A, Patil CK, Campisi J. p38MAPK is a novel DNA damage response-independent regulator of the senescence-associated secretory phenotype. EMBO J 2011;30:1536–1548. [PubMed: 21399611]
24. Arwert EN, Hoste E, Watt FM. Epithelial stem cells, wound healing and cancer. Nat Rev Cancer 2012;12:170–180. [PubMed: 22362215]
25. Hanahan D, Coussens LM. Accessories to the crime: functions of cells recruited to the tumor microenvironment. Cancer Cell 2012;21:309–322. [PubMed: 22439926]
26. Kim C, Sano Y, Todorova K, Carlson BA, Arpa L, Celada A, et al. The kinase p38 alpha serves cell type-specific inflammatory functions in skin injury and coordinates pro- and anti-inflammatory gene expression. Nat Immunol 2008;9:1019–1027. [PubMed: 18677317]
27. Ritprajak P, Hayakawa M, Sano Y, Otsu K, Park JM. Cell type-specific targeting dissociates the therapeutic from the adverse effects of protein kinase inhibition in allergic skin disease. Proc Natl Acad Sci U S A 2012;109:9089–9094. [PubMed: 22615377]
28. Otsuka M, Kang YJ, Ren J, Jiang H, Wang Y, Omata M, et al. Distinct effects of p38alpha deletion in myeloid lineage and gut epithelia in mouse models of inflammatory bowel disease. Gastroenterology 2010;138:1255–1265. [PubMed: 20080092]
29. Cerezo-Guisado MI, del Reino P, Remy G, Kuma Y, Arthur JS, Gallego-Ortega D, et al. Evidence of p38gamma and p38delta involvement in cell transformation processes. Carcinogenesis 2011;32:1093–1099. [PubMed: 21558321]
30. Kwong J, Chen M, Lv D, Luo N, Su W, Xiang R, et al. Induction of p38delta expression plays an essential role in oncogenic ras-induced senescence. Mol Cell Biol 2013;33:3780–3794. [PubMed: 23878395]
31. Demehri S, Turkoz A, Manivasagam S, Yockey LJ, Turkoz M, Kopan R. Elevated epidermal thymic stromal lymphopoietin levels establish an antitumor environment in the skin. Cancer Cell 2012;22:494–505. [PubMed: 23079659]
32. Hu B, Castillo E, Harewood L, Ostano P, Reymond A, Dummer R, et al. Multifocal epithelial tumors and field cancerization from loss of mesenchymal CSL signaling. Cell 2012;149:1207–1220. [PubMed: 22682244]

33. Strickland JE, Dlugosz AA, Hennings H, Yuspa SH. Inhibition of tumor formation from grafted murine papilloma cells by treatment of grafts with staurosporine, an inducer of squamous differentiation. Carcinogenesis 1993;14:205–209. [PubMed: 8435862]
34. Rutberg SE, Adams TL, Glick A, Bonovich MT, Vinson C, Yuspa SH. Activator protein 1 transcription factors are fundamental to v-rasHa-induced changes in gene expression in neoplastic keratinocytes. Cancer Res 2000;60:6332–6338. [PubMed: 11103794]
35. Lin AW, Lowe SW. Oncogenic ras activates the ARF-p53 pathway to suppress epithelial cell transformation. Proc Natl Acad Sci U S A 2001;98:5025–5030. [PubMed: 11309506]
36. Guinea-Viniegra J, Zenz R, Scheuch H, Jimenez M, Bakiri L, Petzelbauer P, et al. Differentiation-induced skin cancer suppression by FOS, p53, and TACE/ADAM17. J Clin Invest 2012;122:2898–2910. [PubMed: 22772468]
37. de Guzman SC, Conlan S, Deming CB, Cheng J, Sears KE, Segre JA. A milieu of regulatory elements in the epidermal differentiation complex syntenic block: implications for atopic dermatitis and psoriasis. Hum Mol Genet 2010;19:1453–1460. [PubMed: 20089530]
38. Glick AB, Yuspa SH. Tissue homeostasis and the control of the neoplastic phenotype in epithelial cancers. Semin Cancer Biol 2005;15:75–83. [PubMed: 15652452]
39. Getsios S, Simpson CL, Kojima S, Harmon R, Sheu LJ, Dusek RL, et al. Desmoglein 1-dependent suppression of EGFR signaling promotes epidermal differentiation and morphogenesis. J Cell Biol 2009;185:1243–1258. [PubMed: 19546243]
40. Lehen'kyi V, Shapovalov G, Skryma R, Prevarskaya,N. Ion channnels and transporters in cancer. 5. Ion channels in control of cancer and cell apoptosis. Am J Physiol Cell Physiol 2011;301:C1281–C1289. [PubMed: 21940667]
41. de Visser KE, Eichten A, Coussens LM. Paradoxical roles of the immune system during cancer development. Nat Rev Cancer 2006;6:24–37. [PubMed: 16397525]
42. Balkwill FR, Mantovani A. Cancer-related inflammation: common themes and therapeutic opportunities. Semin Cancer Biol 2012;22:33–40. [PubMed: 22210179]
43. Kang YJ, Otsuka M, van den Berg A, Hong L, Huang Z, Wu X, et al. Epithelial p38alpha controls immune cell recruitment in the colonic mucosa. PLoS Pathog 2010;6:e1000934. [PubMed: 20532209]
44. Chang S, Iversen L, Kragballe K, Arthur JS, Johansen C. Mice lacking MSK1 and MSK2 show reduced skin tumor development in a two-stage chemical carcinogenesis model. Cancer Invest 2011;29:240–245. [PubMed: 21314333]
45. Scortegagna M, Cataisson C, Martin RJ, Hicklin DJ, Schreiber RD, Yuspa SH, et al. HIF-1alpha regulates epithelial inflammation by cell autonomous NFkappaB activation and paracrine stromal remodeling. Blood 2008;111:3343–3354. [PubMed: 18199827]
46. Scortegagna M, Martin RJ, Kladney RD, Neumann RG, Arbeit JM. Hypoxia-inducible factor-1alpha suppresses squamous carcinogenic progression and epithelial-mesenchymal transition. Cancer Res 2009;69:2638–2646. [PubMed: 19276359]
47. Cipolat S, Hoste E, Natsuga K, Quist SR, Watt FM. Epidermal barrier defects link atopic dermatitis with altered skin cancer susceptibility. Elife 2014;3:e01888. [PubMed: 24843010]
48. Di PM, Nowell CS, KochU, Durham AD, Radtke F. Loss of cutaneous TSLP-dependent immune responses skews the balance of inflammation from tumor protective to tumor promoting. Cancer Cell 2012;22:479–493. [PubMed: 23079658]
49. Biozzi G, Ribeiro OG, Saran A, Araujo ML, Maria DA, De Franco M, et al. Effect of genetic modification of acute inflammatory responsiveness on tumorigenesis in the mouse. Carcinogenesis 1998;19:337–346. [PubMed: 9498286]
50. Castoldi L, Golim MA, Filho OG, Romagnoli GG, Ibanez OC, Kaneno R. Enhanced natural killer activity and production of pro-inflammatory cytokines in mice selected for high acute inflammatory response (AIRmax). Immunology 2007;120:372–379. [PubMed: 17163963]
51. Del Reino P, Alsina-Beauchamps D, Escos A, Cerezo-Guisado MA, Risco A, Aparicio N, et al. Pro-oncogenic role of alternative p38 Mitogen-activated protein kinases p38gamma and p38delta, linking inflammation and cancer in colitis-associated colon cancer. Cancer Res 2014;74:6150–6160. [PubMed: 25217523]

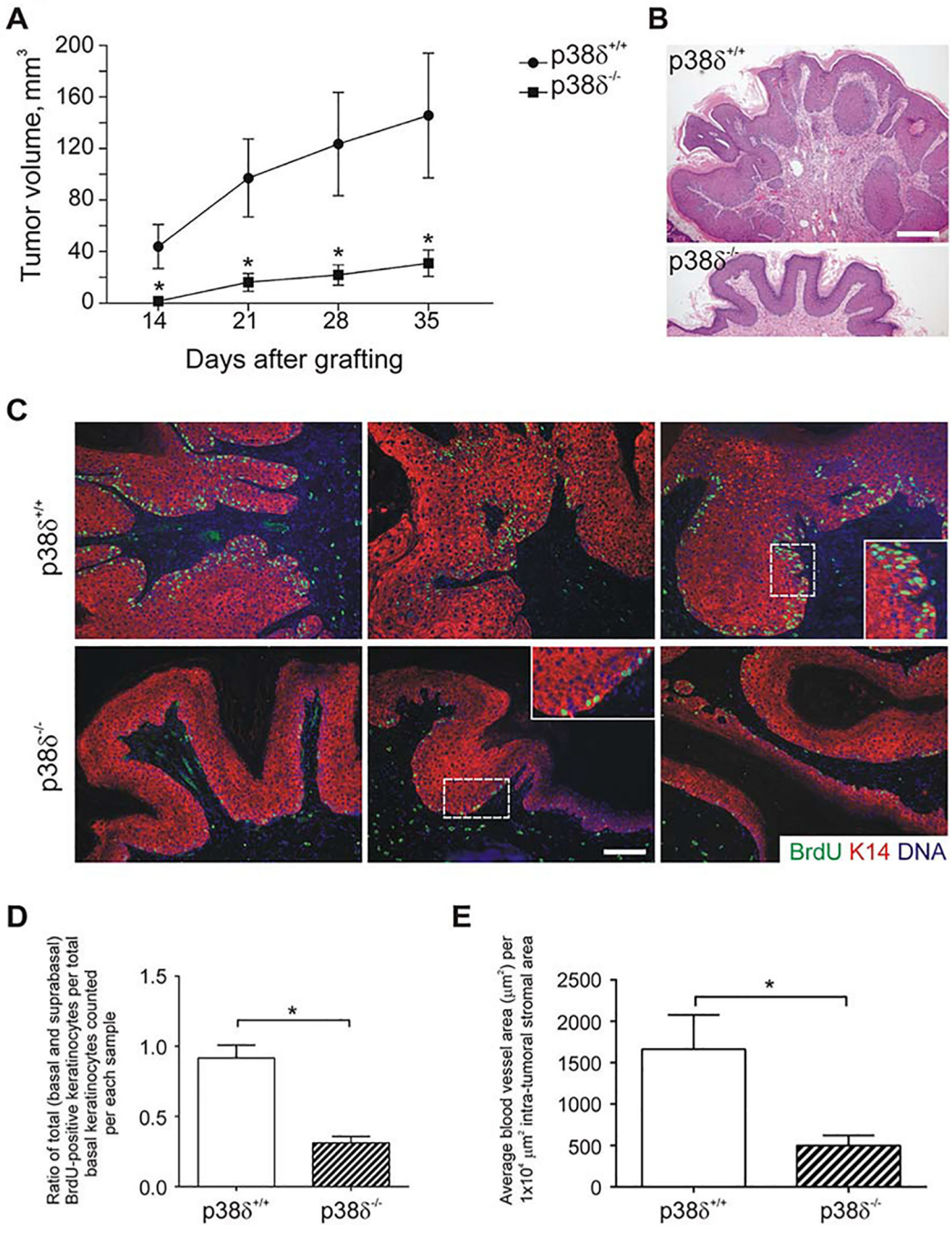

Figure 1. p38δ ablation impairs growth of v-ras^{Ha}-induced squamous tumors.

(**A**) p38δ$^{+/+}$ and p38δ$^{-/-}$ primary v-ras^{Ha}-transduced keratinocytes combined with wild-type fibroblasts were grafted onto nude mice. Tumor dimensions were measured weekly; approximate tumor volumes were determined by multiplying tumor length x width x height. Data were analyzed using GraphPad Prism software and significant values were assigned using one-way ANOVA. *Points*, mean; *bars*, SE. *$P < 0.05$ compared with wild-type for the same time point. Each group contained 10 mice. The results are representative of two independent experiments. Similar levels of Ras expression were confirmed for the two

keratinocyte genotypes by immunoblot (*data not shown*). (**B**) Representative H&E-stained sections from papillomas developed from v-ras^{Ha}-transformed p38δ$^{+/+}$ and p38δ$^{-/-}$ keratinocytes. Scale bar, 250μm. (**C**) Tumor sections were immunostained with the antibodies against BrdU (green) and Keratin 14 (K14, red). Nuclei were counterstained with Hoechst dye (DNA). Four p38δ$^{+/+}$ and four p38δ$^{-/-}$ papillomas were examined. Representative tissue fields from three individual tumors of each genotype are shown. Scale bar, 100μm. Insets show the enlarged images of the areas demarcated by the dashed line in the corresponding panel. (**D**) BrdU incorporation in tumors from v-ras^{Ha}-transformed p38δ$^{+/+}$ and p38δ$^{-/-}$ keratinocytes was compared by scoring the numbers of total (basal and suprabasal) BrdUpositive keratinocytes per a total of 240 basal keratinocytes for each tumor sample in tumor tissue sections immunostained with antibody against BrdU. Data are reported as mean ± SE; n = 5 (p38δ$^{+/+}$ tumors), n = 3 (p38δ$^{-/-}$ tumors). *$P < 0.05$. (**E**) Quantitative analysis of the blood vessel areas in tumors developed from v-ras^{Ha}-transformed p38δ$^{+/+}$ and p38δ$^{-/-}$ keratinocytes. Data are reported as mean ± SE; n = 4 (p38δ$^{+/+}$ tumors), n = 3 (p38δ$^{-/-}$ tumors). *$P < 0.05$.

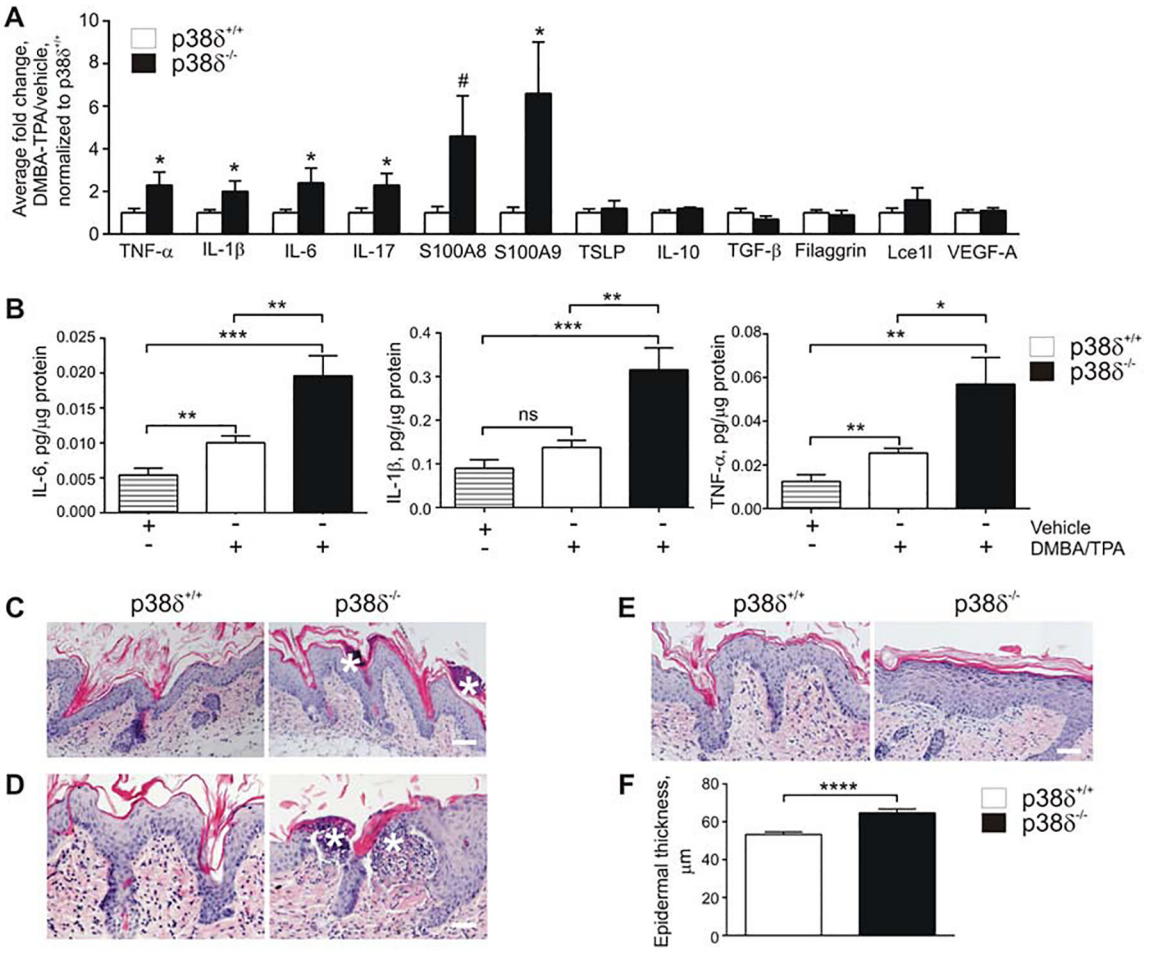

Figure 2. Increased inflammatory cytokine expression and production, and exacerbated inflammation in p38δ$^{-/-}$ skin following a short-term DMBA/TPA challenge.

Sets of p38δ$^{+/+}$ and p38δ$^{-/-}$ littermates were subjected to a topical short-term DMBA/TPA treatment as detailed in the Materials and Methods. Total RNA (**A**) or total skin lysates (**B**) were isolated from full-thickness dorsal skin of mice (acetone vehicle control: n = 9; DMBA/TPA: n = 8–11 per genotype for RNA isolation; n = 10 per genotype for protein isolation) 2 hours after the final TPA application, and the levels of RNA or protein expression of the indicated mediators were analyzed using qRT-PCR (**A**) or ELISA (**B**), respectively. (**A**) qRT-RCR data from DMBA/TPA-treated skin are shown as fold changes over vehicle-treated skin and normalized to values from control p38δ$^{+/+}$ mice. Results in (**A**) and (**B**) are shown as mean ± SE. *P < 0.05, **P < 0.01, ***P < 0.001, # approaching significance at P = 0.0542; ns, not significant; vehicle-treated group included mice of both genotypes. (**C-F**) A short-term DMBA/TPA challenge leads to exacerbated inflammation and increased epidermal thickness in skin of p38δ-null mice. (**C-E**), Representative H&E-stained sections of p38δ$^{+/+}$ and p38δ$^{-/-}$ skin 6 hours after the final TPA application; asterisks, Munro microabscesses (**C**), intraepidermal abscesses (**D**). (**E**) p38δ$^{-/-}$ mice develop significantly increased epidermal thickness in response to DMBA/TPA challenge in comparison to control p38δ$^{+/+}$ mice. Equal epidermal thickness was observed in skin of vehicle-treated mice (not shown). (**F**) Epidermal thickness was measured in six mice per

genotype obtained from two sets of littermates. Five measurements of the epidermal thickness per each of the three randomly selected 20x fields per each animal were included in the analysis, and the mean epidermal thicknesses were compared for p38δ$^{+/+}$ and p38δ$^{-/-}$ mice (n = 6 for each genotype). $^{**}P = 0.0043$, Mann-Whitney test, one-tailed. Scale bars, 100μm (**C**), 50μm (**D, E**).

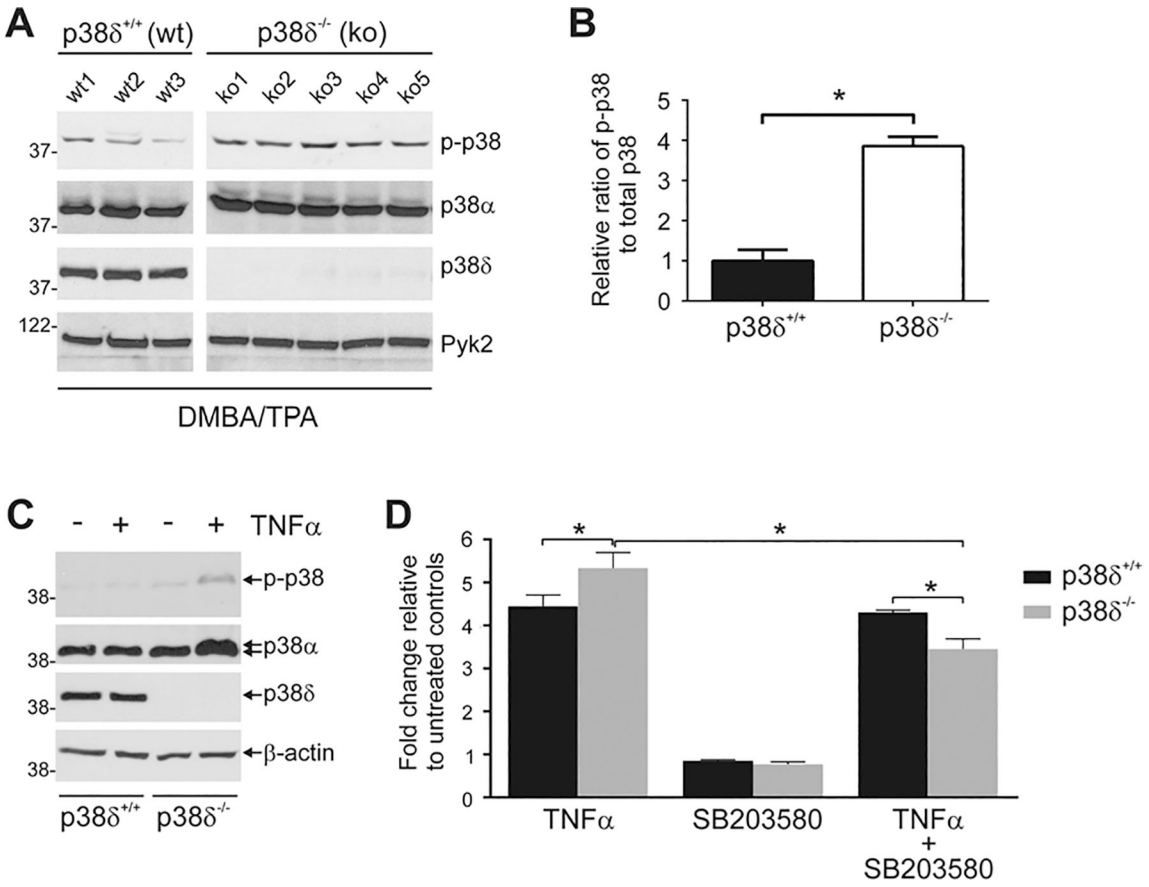

Figure 3. Enhanced activation of p38α signaling in p38δ$^{-/-}$ skin in response to a short-term DMBA/TPA regimen, and in p38δ$^{-/-}$ keratinocytes in response to TNFα.

(**A**) Total skin lysates were isolated from full-thickness dorsal skin of the individual p38δ$^{+/+}$ and p38δ$^{-/-}$ mice 6 hours after the final TPA application, and expression of the indicated proteins was analyzed by immunoblot using the specified antibodies. p-p38, phosphorylated p38 MAPK. Pyk2 levels were assayed to assure equal protein loading. (**B**) Densitometric quantification of phosphorylated p38 bands. Data are normalized to the density of the total p38 bands (comprising p38α and p38δ bands in p38δ$^{+/+}$ skin and p38α band only in p38δ$^{-/-}$ skin). *$P < 0.05$. (**C**) Cultured mouse keratinocytes from newborn p38δ$^{+/+}$ and p38δ$^{-/-}$ littermates were treated with either DMSO vehicle (−) or 20 ng/ml TNFα (+) for 15 min. Total cell lysates were prepared, and immunoblot analysis was carried out using the antibodies specific for the indicated proteins. A slightly lower motility (higher molecular weight) band on the p38α immunoblot corresponds to the phosphorylated form of p38α (upper arrow, p38α blot). β-actin levels were assayed as a loading control. (**D**) p38δ$^{+/+}$ and p38δ$^{-/-}$ keratinocytes were transfected with a NFκB luciferase reporter construct, treated as described in the Materials and Methods, harvested and assayed for luciferase activity. Bars, mean ± SE. *$P \leq 0.05$. Results are representative of two independent experiments performed in triplicate using keratinocytes isolated from newborn epidermis from sets of littermates (n = 4 per each genotype per experiment), pooled prior to plating.

Table 1.

Changes in the expression of selected genes in oncogenic v-ras^{Ha}-transformed p38δ-null keratinocytes, compared to v-ras^{Ha}-transformed control keratinocytes, by microarray analysis. Shown ontological categories are differentially expressed at a significant level (*P*-values ranging from 10^{-17} to 10^{-5}). Gene expression differences for selected genes were validated by qRT-PCR (as described in the text, and data not shown). Among the down-regulated genes, those additionally linked to vasculature development/angiogenesis are denoted in bold.

Categories	Up (↑) / Down (↓)	Genes
Keratinocyte Differentiation/ Keratinization/ Cornified Envelope/ Small Proline-Rich	↑	LOR, HRNR, SPRR2D, FLG, RPTN, CNFN, SPRR2H, SPRR2G, SPRR2F, SPRR2E, SPRR2K, SPRR2I, LCE1B, SPRR2K, LCE1I, LCE1F, LCE1C, LCE1D, SPRR4, LCE1A1, LCE1A2, LCE1L
Cell Adhesion	↑	DSG1C, DSG1B, PKP4, DSC1, CLDN15, PCDH7, CDH23, DST/BPAG1
Gap Junction	↑	GJB5, GJB6, GJA4, GJC2, GJA3, GJB2
Ion Channel	↑	CLCN1, KCNMB4, FXYD4, GRIK1, SHROOM4, GABRB3, GABRB2, KCNAB1, GRIK2, GRIK3,CACNB1, KCNA3, ATP12A, KCNJ2, KCNJ3, KCNK12, KCNMB2, GRID2, SCNN1B, HCN3, SCN10A, TRPC2, KCND3, GABRA4, CLCA3, KCNK4, ITPR2, P2RX5, CATSPER4, KCNJ6, GRIA2, KCNN2, KCNF1, KCNH2, SCN4A, ATP7B
Cell Proliferation	↓	FGF5, NOG, FOSL2, FGF15, **FGF9**, PTGS1, NR2E3, MEN1, BDNF, OSR2, CDKN2A, **MYOCD**, WDR77, TICAM1, RARB, ASPH, FANCA, LTB, DLG1, CD3E, LOC100046643, SIX5, FGF21, **PROX1**, IL20RB, TNFSF13B, CCND2, ZMIZ1, GHRL, LOC100047930, **PML**, PPT2, CD24A, **HOXA3**, **OVOL2**, RAC2, TRP53, TCF7, **NF2**, KLF10, **TGFBR2**, **NF1**, DUSP22, LOC100046825, TAX1BP3, LOC100047603, FOXP2, **KDR**, NOTCH2, FCGR2B, TSC1, IRF6, GKN1, LOC100045958, HTR2A
Receptor Protein Tyrosine Kinase Signaling Pathway	↓	FGF5, PLXNA1, **FGF9**, ERBB3, RGL3, SORCS1, FGF13, BDNF, SOS1, CSF1R, **PTPRJ**, RET, LTK, PIK3CD, CBL, LOC100046643, FGF21, ALK, **KDR**, NTRK3, **SEMA6A**, SEMA6D, DOK5, **PDGFRA**, SEMA4B, CD79B

Table 2.

Statistically enriched groups of the overrepresented functionally related genes, up- regulated (**A**) or down-regulated (**B**, selected groups are shown) in v-ras^{Ha}-transformed p38δ-null keratinocytes, compared to v-ras^{Ha}-transformed p38δ$^{+/+}$/p38δ$^{+/-}$ control keratinocytes. 1.98 was used as a cutoff for enrichment scores.

A	**Enrichment Score: 5.74**	**Count**	**PValue**	**Bonferroni**
	3 45.2 cM	9	2.21E-08	2.55E-05
	keratinization	12	5.57E-08	2.79E-05
	epidermal cell differentiation	13	1.49E-04	3.34E-01
	Enrichment Score: 3.40			
	passive transmembrane transporter activity	46	1.49E-04	1.24E-01
	channel activity	46	1.49E-04	1.24E-01
	Enrichment Score: 2.26			
	sodium channel complex	6	1.29E-03	4.15E-01
	sodium channel	7	1.08E-02	9.96E-01
	Enrichment Score: 2.08			
	cell adhesion	42	2.95E-03	7.73E-01
	biological adhesion	54	1.39E-02	1.00E+00
	Enrichment Score: 2.02			
	CONNEXIN	6	5.35E-03	9.82E-01
	Gap junction	6	7.20E-03	7.79E-01
B	**Enrichment Score: 2.71**	**Count**	**PValue**	**Bonferroni**
	regulation of kinase activity	28	9.58E-04	9.50E-01
	regulation of protein kinase activity	27	1.29E-03	9.82E-01
	Enrichment Score: 2.49			
	guanine-nucleotide releasing factor	19	2.90E-04	1.37E-01
	Guanyl-nucleotide exchange factor	17	2.60E-02	9.97E-01
	Enrichment Score: 2.26			
	blood vessel development	32	2.26E-03	9.99E-01
	vasculature development	32	3.29E-03	1.00E+00
	Enrichment Score: 2.19			
	small GTPase binding	11	9.01E-03	1.00E+00
	Ras GTPase binding	10	2.01E-02	1.00E+00
	Enrichment Score: 2.06			
	egf-like domain	29	2.30E-03	6.88E-01
	EGF-like	25	1.03E-02	1.00E+00
	Enrichment Score: 1.98			
	transmembrane receptor protein tyrosine kinase activity	12	1.92E-03	8.25E-01
	TYROSINE PROTEIN KINASE	15	3.52E-03	9.36E-01